Available online at www.sciencedirect.com
ScienceDirect
Coordination Chemistry Reviews 251 (2007) 12–24
COORDINATION CHEMISTRY REVIEWS
www.elsevier.com/locate/ccr

Review

The study of the ground state Kramers doublet of low-spin heminic system revisited A comprehensive description of the EPR and Mössbauer spectra

Pablo J. Alonso *, Jesús I. Martínez, Inés García-Rubio [1]

Instituto de Ciencia de Materiales de Aragón (Consejo Superior de Investigaciones Científicas-Universidad de Zaragoza), Pza. S. Francisco s/n, E-50009 Zaragoza, Spain

Received 1 March 2006; accepted 12 May 2006
Available online 19 May 2006

Contents

Abstract

A general study of the ground state Kramers doublet of Fe^{III} in the low-spin configuration using the hole formalism is presented. This description allows a generalization of Taylor equations that relate *g*-values of iron to the wave function of the unpaired electron and the energy separation between the t_{2g} orbitals. Expressions for the Fe-hyperfine tensor and valence contribution to the ^{57}Fe nuclear quadrupolar interaction are also obtained for the general case. The model is connected with the counter-rotation effect described in heme systems, which appears in the formulation as a particular case. A procedure to analyze data from EPR and Mössbauer spectroscopic techniques together is presented. It lets us distinguish between the two essentially different solutions derived when only EPR data are available. The model is applied to experimental results available in the literature.

Keywords: Electronic structure; EPR spectroscopy; Heme complexes; Low-spin iron(III); Mössbauer spectroscopy

1. Introduction

Cytochromes and other low-spin hemeproteins are ubiquitous in living organisms. Many relevant properties of their biochemical functions (for example as charge carriers) are determined by the structure and electronic distribution of the heme centers. It is generally accepted that the heme axial ligands play a crucial role in determining them.

The structure and electronic properties in relation to the function of these systems has been studied by means of different spectroscopic techniques including electron paramagnetic resonance (EPR) and Mössbauer. When the protein structure is known, it can be connected with the spectroscopic results. However, as Walker pointed out [1], there are still a great number of

* Corresponding author. Tel.: +34 976 761333; fax: +34 976 761229.
E-mail address: alonso@unizar.es (P.J. Alonso).
[1] Current address: Laboratory of Physical Chemistry, ETH Hönggerberg, CH-8093 Zürich, Switzerland.

0010-8545/$ – see front matter © 2006 Elsevier B.V. All rights reserved.
doi:10.1016/j.ccr.2006.05.007

these systems that cannot yet be structurally characterized. An alternative approach has been the use of synthetic heme centers as model compounds of the prosthetic group of hemeproteins. For these reasons, a large amount of spectroscopic information on different low-spin Fe^{III} systems is available. It has been collected in different reviews [1–4].

In this context the Griffith model is used for analyzing EPR and Mössbauer results [5]. This model is a particularization of the formalism developed by Bleaney and O'Brien [6]. The electronic ground state is determined predominantly by the cubic contribution to the crystal field while additional axial and rhombic contributions (related with heme axial ligands) are treated as a perturbation. Later Taylor published the equations that have been extensively used for deriving the wave function of the unpaired electron from the principal values of the *g*-tensor obtained by EPR spectroscopy [7].

On the basis of the Taylor model, and following the ideas developed by Oosterhuis and Lang [8], the hyperfine (hf) tensor as well as the valence contribution to the electric field gradient (EFG) at the iron nucleus have been estimated in order to account for the Mössbauer spectra of some low-spin Fe^{III} systems [1–4]. It is worth noting that the formal equations that give the hf coupling constants were obtained under the implicit assumption of common principal axes for all *g*, hf and EFG tensors in spite of the fact that a freedom of rotation has been considered for fitting the Mössbauer data in some cases [9,10].

In order to take account of this rotation, the orientation of the magnetic (principal *g*-tensor) axes with respect to the molecule frame has to be determined. This problem has been considered in the past by several authors. Byrn et al. [11] introduced the counter-rotation concept and later Shokhirev and Walker [12] discussed this point by considering the effect of the excited orbitals in the Fe^{III} ground state ones due to the low symmetry crystal field and the spin-orbit contributions. In particular, it is generally accepted that in most low-spin heme systems one of the *g*-tensor axes (namely the *Z*-axis) is nearly normal to the heme plane, whereas the *X*- and *Y*-axes are rotated with respect to the molecular axes (*x*, *y*) defined by the N–Fe bonding directions in the porphyrin plane. So, in this particular case the orientation of the magnetic axes is defined by the angle γ that the *X*- and *x*- (or *Y* and *y*-) axes make (see Fig. 1). This situation has been confirmed in those systems where single crystal EPR data are available. In spite of that, in some studies where Taylor's equations are applied, molecular axes are used and the principal *x*- and *y*-axes of all *g*, hf and EFG tensors are assumed to coincide and be directed along the Fe–N directions [3,13].

So, it will be useful to develop a more general description of the ground state electronic properties of these Fe^{III} (d^5) systems in order to give a formulation that includes the hf and EFG in addition to the *g* tensor when the magnetic axes differ from the molecular axes. In the early work by Bleaney and O'Brien this question was considered in two particular cases [6]. The authors only took into account the Zeeman and hyperfine interaction and they already pointed out that the *g* and hf tensor may be non-coaxial which makes it difficult to calculate the principal direction of the hf tensor. On the other hand McGarvey, in a recent paper [14], has reviewed the *g* tensor formulation for strong field

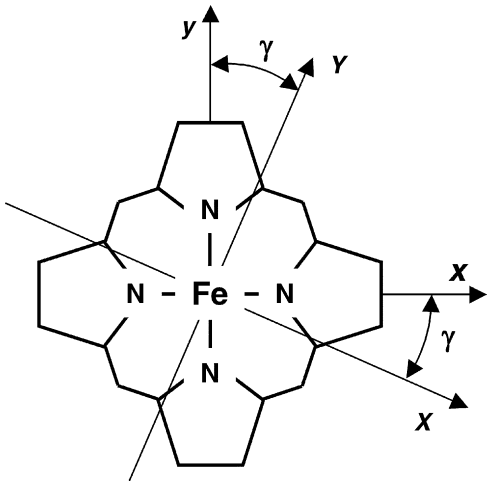

Fig. 1. Sketch of the heme moiety showing the molecular *x*- and *y*-axes. The molecular *z*-axis is normal to the heme plane. The magnetic *X*- and *Y*-axes are also depicted. The magnetic *Z*-axis coincides with the molecular *z*-axis. The rotation angle γ is also shown.

d^5 systems. This author has noted that "although it was done correctly in the beginning by Bleaney and O'Brien many confusing and not ever correct versions have been employed since". In particular, this author used a five electron Slater determinants formulation in order to manage the spin–orbit coupling with the e_g excited states for accounting for the second-order *g*-shift, which could be most significant in $4d^5$ and $5d^5$ low-spin systems. [14]. Moreover, he also indicated that since only the magnitude of the principal *g*-values are determined from the EPR data, two different solutions in term of crystal field parameters that correspond to a very different unpaired electron distribution are obtained [7,14–16]. They can be distinguished when the sign of the product of the three principal *g*-values (the determinant of the *g*-tensor) is known, for instance, in an EPR experiment using circular polarized microwave excitation [17]. Nevertheless, results of such an experiment have not been reported in low-spin Fe^{III} systems. In one case, Huynh et al. [16] took advantage of the hyperfine coupling with the ^{57}Fe nucleus determined by Mössbauer spectroscopy to prove that the product of the three principal *g*-values is positive in the case of Cytochrome c_2 from *Rhodospirillum rubrum*.

With all these considerations we have revisited the Griffith formulation with the aim of giving a comprehensive description that includes the *g*, hf, and EFG tensor in a general situation where the principal axes of these coupling tensors are not coincident and thus apart from the molecular (*x*, *y*, *z*) axes. The equations giving the principal *g*-tensor values formally coincident with those obtained by Taylor [7] will be derived in our description. This coincidence prevents obtaining information about magnetic axes orientation in disordered samples when only principal *g*-values are available. We will also conclude that the hyperfine and EFG coupling tensors provide information about the orientation of the principal axes of the relevant tensor and also let us discriminate between the two possible solutions derived from a conventional EPR experiment. Consequently,

valuable information about the unpaired electron orbital can be obtained in this way.

This general result will be particularized to the common situation where the normal to the heme ring is a principal axis of the g-tensor (namely the Z-axis) and the orientation of the magnetic axes is just given by one angle γ (see above). In this case closed expressions for all the tensors will be given. Some experimental data will be analyzed showing that information about the orientation of all tensors (and precise information about the unpaired electron orbital) can be obtained by combining EPR and Mössbauer results.

2. Theoretical background

2.1. Description of the ground state Kramers doublet

In a low-spin ferric heme system, the electronic ground state is determined by the effect of the crystal field on the d^5 configuration of the Fe^{III} ion. It is currently assumed that the strong crystal field scheme is suitable for describing its electronic properties, the octahedral crystal field contribution being the dominant one. Then, the five 'd' electrons of the Fe^{III} ions must be placed in the six available orbitals in the t_{2g} triplet and, consequently, the ground state can be described simply by specifying the unique unoccupied orbital (hole formalism). Thus, the problem is reduced to the study of a single particle. The low symmetry contributions to the crystal field and the spin–orbit are included in a first-order approximation [5].

Taylor, in a classical paper [7], studied a particular situation in detail. There the octahedral distortions take place along the N–Fe bonding directions. So, the system preserves a C_{2v} symmetry and the electronic orbitals coincide with the standard d-orbitals $\{d_{yz}, d_{zx}, d_{xy}\}$. For convenience, in the following we will use the notation:

$$\varphi^{(X)} = d_{yz}, \qquad \varphi^{(Y)} = d_{zx}, \qquad \varphi^{(Z)} = d_{xy}, \tag{1}$$

and, as it is usual, the splitting of the orbital energies will be parameterized by two crystal field parameters Δ and V.

When the spin–orbit interaction is included, the ground state for the electronic hole turns out to be a Kramers doublet, which is spanned by

$$\psi_1 = a\varphi^{(X)}\alpha - \mathrm{i}b\varphi^{(Y)}\alpha - c\varphi^{(Z)}\beta,$$
$$\psi_2 = a\varphi^{(X)}\beta + \mathrm{i}b\varphi^{(Y)}\beta + c\varphi^{(Z)}\alpha, \tag{2}$$

where α and β are, respectively, the spin states $m_s = +1/2$ and $m_s = -1/2$ with respect to the z-axis. The (a, b, c) coefficients that define the ground state fulfill the normalization condition, $a^2 + b^2 + c^2 = 1$ and are related to the crystal field parameters Δ and V by

$$\frac{\Delta}{\zeta} = \frac{1}{4}(a+b+c)\left\{\frac{2}{c} - \frac{1}{a} - \frac{1}{b}\right\},$$
$$\frac{V}{\zeta} = \frac{1}{2}(a+b+c)\left\{\frac{1}{b} - \frac{1}{a}\right\}, \tag{3}$$

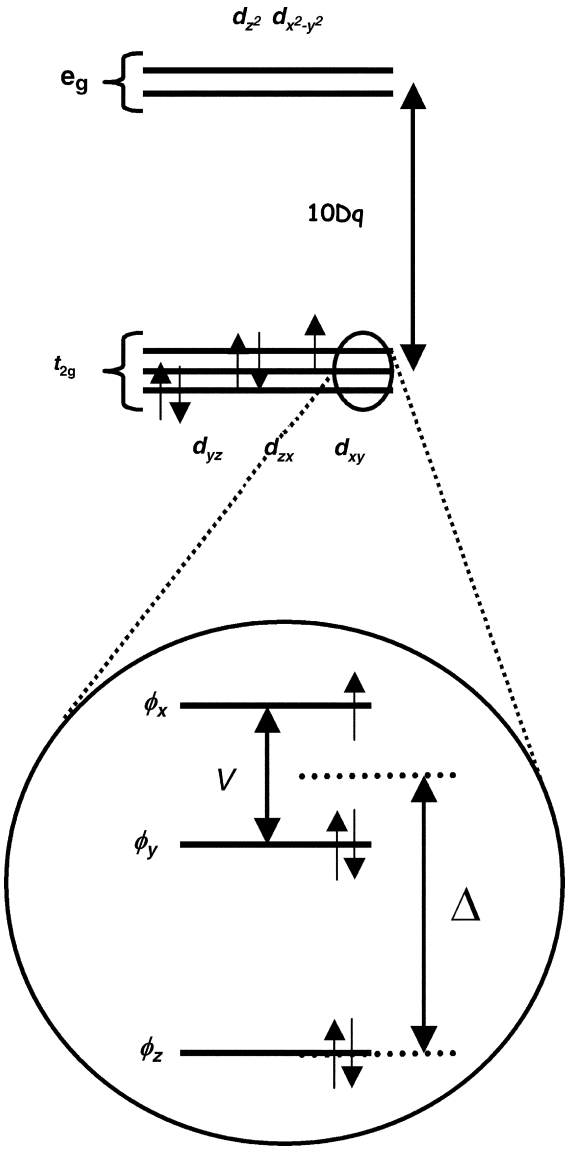

Fig. 2. Splitting of the d-orbitals in absence of the spin–orbit coupling, when the effect of the low symmetry contributions is small compared with the cubic 10 Dq contribution. Allocation of the five electrons of Fe^{III} is indicated.

ζ being the spin–orbit coupling constant [7]. Note that ψ_1 and ψ_2 are a pair of Kramers conjugate states and under time inversion they transform as the $|+1/2\rangle$ and $|-1/2\rangle$ states of a $S = \frac{1}{2}$ system does [18].

By taking into account the Zeeman interaction, Taylor also provides equations that relate the principal g values to the (a, b, c) coefficients. In this way an estimation of the Δ/ζ and V/ζ quotients can be obtained from the EPR data.

Let us now consider a general situation outlined in Fig. 2. Again, the low symmetry effects of the crystal field produce the splitting of the t_{2g} orbitals, which can still be parameterized as a function of two crystal field parameters Δ and V. However, in general the crystal field orbital wave functions $\{\phi_X, \phi_Y, \phi_Z\}$ do not coincide with the standard d-orbitals (1). As long as the low symmetry crystal field effects are included in a first-order approximation, these orbital wave functions $\{\phi_X, \phi_Y, \phi_Z\}$ are

given as a linear combination of the standard ones $\{\varphi^{(X)}, \varphi^{(Y)}, \varphi^{(Z)}\}$:

$$\begin{pmatrix} \phi_X \\ \phi_Y \\ \phi_Z \end{pmatrix} = \Omega \begin{pmatrix} d_{yz} \\ d_{xz} \\ d_{xy} \end{pmatrix} = \Omega \begin{pmatrix} \varphi^{(X)} \\ \varphi^{(Y)} \\ \varphi^{(Z)} \end{pmatrix}. \quad (4)$$

In principle, Ω is a unitary matrix, as it transforms a basis of the t_{2g} triplet into another one, but it will be real orthogonal because it relates real wave functions. A suitable election of the phase of the wave functions $\{\phi_X, \phi_Y, \phi_Z\}$ leads to $\det(\Omega) = +1$. Thus, Ω can be chosen as a real direct orthogonal matrix $\Omega \in O^+(3)$. In other words, it represents a rotation in the three dimensional space. Consequently, we can use Ω to define a new reference frame (X, Y, Z) by

$$\begin{pmatrix} X \\ Y \\ Z \end{pmatrix} = \Omega \begin{pmatrix} x \\ y \\ z \end{pmatrix}. \quad (5)$$

The X, Y, Z axes will be called magnetic axes. We will see that these new axes are the principal axes of the g tensor that describe the magnetic properties. A reordering of $\{\phi_X, \phi_Y, \phi_Z\}$ translates into an ambiguity of the ordering of the X, Y, Z magnetic axes. However, when the canonical condition $0 \le V \le 2|\Delta|/3$ is fulfilled, this ambiguity is removed. This canonical condition leads to the selection of the proper axes for the magnetic axes. However, in some cases the proper axes are not selected for the description of the magnetic properties of heme compounds and the Z-axis practically coincides with the normal to the heme plane [10]. This point will be dealt with in detail later.

On the other hand, Bleaney and O'Brien [6] already noted that the reference frame corresponding to the magnetic axes satisfies:

$$\langle\phi_k|L_X|\phi_l\rangle = \langle\varphi^{(k)}|L_x|\varphi^{(l)}\rangle, \qquad \langle\phi_k|L_Y|\phi_l\rangle = \langle\varphi^{(k)}|L_y|\varphi^{(l)}\rangle,$$
$$\langle\phi_k|L_Z|\phi_l\rangle = \langle\varphi^{(k)}|L_z|\varphi^{(l)}\rangle \quad (k, l = X, Y, Z), \quad (6)$$

where the notation given in (1) has been used.

This means that the values for the orbital angular moment with respect to the magnetic axes (X, Y, Z) obtained using the crystal field wave functions $\{\phi_X, \phi_Y, \phi_Z\}$ are the same as those obtained using the standard orbital wave functions $\{\varphi^{(X)}, \varphi^{(Y)}, \varphi^{(Z)}\}$ in the molecular axes (x, y, z). This result allows the problem of including the spin–orbit perturbation and finding the ground state Kramers doublet to be reformulated in the magnetic axes in a similar way as in the situation described by Taylor [7]. So, introducing the spin functions $\{\alpha', \beta'\}$ corresponding to $m_s = +1/2$ and $m_s = -1/2$, respectively (with respect to the Z-axis), the basis of the ground state Kramers doublet is given by

$$\psi_1 = a\phi_X\alpha' - \mathrm{i}b\phi_Y\alpha' - c\phi_Z\beta',$$
$$\psi_2 = a\phi_X\beta' + \mathrm{i}b\phi_Y\beta' + c\phi_Z\alpha', \quad (7)$$

where the coefficients (a, b, c) are still given as a function of Δ/ζ and V/ζ by Eq. (3) together with the normalization condition. Again ψ_1 and ψ_2 are a pair of Kramers conjugate states and they transform under time inversion as the $|+1/2\rangle$ and $|-1/2\rangle$ states of a $S = \frac{1}{2}$ system.

In addition, the principal values of the g tensor as a function of the (a, b, c) coefficients are also given by Taylor's equations, and it can be proved that the principal axes of the g-tensor coincide with the magnetic axes. This point will be developed in the following paragraphs although these ideas have already been introduced elsewhere [19].

To achieve this, we will make use of the fictitious spin formalism that allows us to handle the ground state Kramers doublet as a $S' = \frac{1}{2}$ system [20]. This is done by the identification of any Kramers conjugate pair of basis states with the standard states $\{|+\rangle, |-\rangle\}$ of a spin 1/2 system and substituting each operator $\hat{O}$, when restricted to the Kramers doublet, by an equivalent operator $\hat{O}_S$ that is expressed as a function of spin operators. In the next sections we will show the substitution of all the relevant operators in the spin Hamiltonian by their equivalent operators. As discussed in Ref. [20] there is some degree of arbitrariness in this identification. In the present work we have chosen the $\{\psi_1 \leftrightarrow |+\rangle, \psi_2 \leftrightarrow |-\rangle\}$ substitution rule. With such an identification the transformation properties of the states under time reversal are preserved. A discussion about this point and the general guidelines for substituting each operator and using the fictitious spin formalism are given in Appendix A.

2.2. Zeeman interaction

The Zeeman interaction corresponds to the interaction with a magnetic field $\vec{B}$ and is given by

$$H_{Ze} = \mu_B \vec{B} \cdot (k\vec{L} + g_e\vec{S}), \quad (8)$$

where μ_B represents the Bohr magneton, g_e the free electron g-factor ($g_e = 2.0023$), and $\vec{L}$ and $\vec{S}$ are the orbital angular moment and true spin operators, respectively. k is the orbital reduction factor that phenomenologically accounts for the covalence effects and the mixing with excited states due to low symmetry contribution to the crystal field [14,15]. Usually it takes a value close to the unity.

The equivalent operator of (8) in the fictitious spin formalism, see Eq. (A.5), is

$$(H_{Ze})_S = \mu_B \vec{B} \cdot \{(k\tilde{\Xi}_L + g_e\tilde{\Xi}_S)\vec{S}'\}, \quad (9)$$

with $S' = \frac{1}{2}$. The tensors $\tilde{\Xi}_L$ and $\tilde{\Xi}_S$ are given in (A.17). Taking into account that both $\tilde{\Xi}_L$ and $\tilde{\Xi}_S$ are symmetric and omitting hereafter the subscript S, the last expression can be written as

$$H_{Ze} = \mu_B \vec{B} \cdot \tilde{g} \cdot \vec{S}', \quad (10)$$

with

$$\tilde{g} = k\tilde{\Xi}_L + g_e\tilde{\Xi}_S. \quad (11)$$

As the tensors $\tilde{\Xi}_L$ and $\tilde{\Xi}_S$ are diagonal in the axes (X, Y, Z), these are also the principal axes of the g tensor, which explains why they are called magnetic axes. Moreover, taking into account (A.17) the principal values of the g tensor are

$$g_X = g_e(a^2 - b^2 - c^2) - 4kbc,$$
$$g_Y = g_e(a^2 - b^2 + c^2) + 4kac,$$
$$g_Z = g_e(a^2 + b^2 - c^2) + 4kab, \tag{12}$$

which reduce to Taylor's formulae by taking $g_e = 2$ and $k = 1$. Now with a correct choice of the sign (remember that EPR experiments only provide their absolute values and occasionally the sign of the product $g_x g_y g_z$) and the order of the principal g values [7], the coefficients that define the ground state can be obtained using the former equations together the normalization condition:

$$a^2 + b^2 + c^2 = 1. \tag{13}$$

Although these expressions are formally the same as those given by Taylor [7], we want to emphasize that when the orientation of the magnetic axes remains unknown (as happens when the EPR spectrum of a non-oriented sample is studied) these coefficients only provide information about the low symmetry parameters Δ/ζ and V/ζ of the crystal field. One does not gain information about the orbital wave functions $\{\phi_X, \phi_Y, \phi_Z\}$, which are defined as a function of the standard d-orbitals by means of the rotation matrix Ω, see (4). This result explains why Taylor's equations are useful for describing the EPR spectra of low-spin Fe(III) systems out of the symmetry conditions of the original paper.

We want to bear in mind, as has been commented above, that two pairs of values of the ratios Δ/ζ and V/ζ can be derived from the measured g-values. These solutions correspond to a different unpaired electron distribution [15,16]. Different physical arguments have been used to distinguish between them [1,4,15] but experimental verifications to support the choice are scarce. The analysis of the hyperfine interaction with the ^{57}Fe nucleus allows us to determine the actual one as was done in a particular case by Huynh et al. [16].

2.3. Hyperfine interaction

When the metal nucleus has a non-zero nuclear spin I (for instance, ^{57}Fe observed in Mössbauer experiments) the hyperfine interaction must be considered. It is done by including in the Hamiltonian the following contribution:

$$H_{hf} = \underbrace{\mu_N g_N \mu_B g_e \left(\frac{1}{r^3} k\vec{L}\right) \cdot \vec{I}}_{H_{hf}^L} + \underbrace{\mu_N g_N \mu_B g_e \left[\frac{1}{r^5}\{3\vec{r}(\vec{r}\cdot\vec{S}) - r^2\vec{S}\}\right] \cdot \vec{I}}_{H_{hf}^S} + \underbrace{\frac{8\pi}{3}\mu_N g_N \mu_B g_e \left[\delta(\vec{r})\vec{S}\right] \cdot \vec{I}}_{H_{hf}^F}, \tag{14}$$

where the orbital, spin, and Fermi contributions H_{hf}^L, H_{hf}^S, H_{hf}^F, respectively, are explicitly indicated [21] and k is the orbital reduction factor previously introduced. Now, the nuclear degrees of freedom have to be included, hence (14) must be evaluated using the base of states given by $\{\psi_1|m\rangle, \psi_2|m\rangle\}$, with $m = -I, \ldots, I$.

The fictitious spin formalism applies straightforwardly to the orbital and Fermi hyperfine contributions. So, using the results outlined in the Appendix, the equivalent operators H_{hf}^L and H_{hf}^F in the Kramers subspace are given by

$$H_{hf}^L = \tilde{S}' \cdot \hat{A}^L \cdot \vec{I} \quad \text{and} \quad H_{hf}^F = \tilde{S}' \cdot \hat{A}^F \cdot \vec{I}, \tag{15}$$

where

$$\hat{A}^L = \mu_N g_N \mu_B g_e \langle r^{-3}\rangle k \tilde{\Xi}_L \quad \text{and}$$
$$\hat{A}^F = \frac{8\pi}{3}\mu_N g_N \mu_B g_e \rho(0) \tilde{\Xi}_S \tag{16}$$

are respectively the orbital and Fermi contributions to the "hyperfine tensor", which can be directly evaluated if the Kramers doublet basis wave function (7) is known. The symbol $\langle r^{-3}\rangle$ is defined in (A.20) and $\rho(0)$ is the value of the $\rho(\vec{r})$ function (A.16) in the iron nucleus. Both $\hat{A}^L$ and $\hat{A}^F$ are symmetric tensors and these two contributions are diagonal in the magnetic axes because the $\tilde{\Xi}_L$ and $\tilde{\Xi}_S$ tensors are diagonal as well. Thus, they do not provide any information about the orientation of the magnetic axis in non-oriented samples. In fact, when the orbital wave functions $\{\phi_X, \phi_Y, \phi_Z\}$ are linear combinations of pure d-orbitals, $\hat{A}^F$ should be zero as long as $\rho(0) = 0$. Non-zero values for $\hat{A}^F$ are observed in experiments and are interpreted as being due to core polarization of the inner s-electrons or to mixing with excited configurations. This can be included in a phenomenological way introducing a non-dimensional parameter κ by [21]:

$$\kappa\langle r^{-3}\rangle = -\frac{8\pi}{3}\rho(0). \tag{17}$$

It should be noted that the Fermi contribution $\hat{A}^F$, which is isotropic in many simpler systems such as a Kramers doublet ground state from an orbital singlet, is here, in general, anisotropic since $\tilde{\Xi}_S$ is anisotropic. Similarly, $\hat{A}^L$ in general does not have zero trace, because $\mathrm{tr}(\tilde{\Xi}_L) = 4(ab + ac - bc)$.

Let us now consider the spin contribution in (14). It can be written as

$$H_{hf}^S = \mu_N g_N \mu_B g_e \left[\frac{1}{r^5}\{\vec{r}(\vec{r}\cdot\vec{S}) - r^2\vec{S}\}\right] \cdot \vec{I} = \mu_N g_N \mu_B g_e (\tilde{\tau}\cdot\vec{S}) \cdot \vec{I}, \tag{18}$$

where $\tilde{\tau}$ is a second rank tensor operator that only depends on the spatial electronic coordinates. Its components are given by

$$\tau_{kj} = \frac{1}{r^5}\{3r_k r_j - \delta_{kj} r^2\}, \tag{19}$$

where $r_k, r_j = x, y, z$ are the coordinates of $\vec{r}$. So, we are in the situation given in (A.7) and the equations following it. Consequently, the equivalent operator of (18) can be written as

$$H_{hf}^S = \tilde{S}' \cdot \hat{A}^S \cdot \vec{I}. \tag{20}$$

Unlike with $\hat{A}^L$ and $\hat{A}^F$, it is not possible to give a closed expression for the spin contribution $\hat{A}^S$ to the hyperfine tensor. Bleaney

and O'Brien obtained it in some particular cases and they also indicated the non-symmetrical character of $\hat{A}^S$ [6]. Here we outline a general procedure to calculate its components in the magnetic coordinate reference frame (X, Y, Z) given a Kramers doublet basis (7).

First note that $\tilde{\tau}$ factors is the product of a scalar operator r^{-3} depending on the radial distance and a second range tensor operator that only includes angular variables (θ, ϕ):

$$\tilde{\tau} = r^{-3} \cdot \tilde{\tau}^{\Omega}(\theta, \phi), \tag{21}$$

where $\tilde{\tau}^{\Omega}$ is given by

$$\tau^{\Omega}_{kj}(\theta, \phi) = \begin{pmatrix} 3\sin^2\theta\cos^2\phi - 1 & 3\sin^2\theta\cos\phi\sin\phi & 3\cos\theta\sin\theta\cos\phi \\ 3\sin^2\theta\cos\phi\sin\phi & 3\sin^2\theta\sin^2\phi - 1 & 3\cos\theta\sin\theta\sin\phi \\ 3\cos\theta\sin\theta\cos\phi & 3\cos\theta\sin\theta\sin\phi & 3\cos^2\theta - 1 \end{pmatrix}. \tag{22}$$

The matrix $\tilde{\tau}^{\Omega}$ can be expressed as a linear combination of spherical harmonics $Y_{kq}(\theta, \phi)$ with $k = 2$.

Now, from (A.4) it follows that

$$\begin{aligned} A^S_{xk} &= \mu_N g_N \mu_B g_e \langle r^{-3}\rangle 2\,\mathrm{Re}\langle\psi_2|\tau^{\Omega}_{kx}S_x + \tau^{\Omega}_{ky}S_y + \tau^{\Omega}_{kz}S_z|\psi_1\rangle, \\ A^S_{yk} &= \mu_N g_N \mu_B g_e \langle r^{-3}\rangle 2\,\mathrm{Im}\langle\psi_2|\tau^{\Omega}_{kx}S_x + \tau^{\Omega}_{ky}S_y + \tau^{\Omega}_{kz}S_z|\psi_1\rangle, \\ A^S_{zk} &= \mu_N g_N \mu_B g_e \langle r^{-3}\rangle 2\langle\psi_1|\tau^{\Omega}_{kx}S_x + \tau^{\Omega}_{ky}S_y + \tau^{\Omega}_{kz}S_z|\psi_1\rangle \\ &(k = x, y, z), \end{aligned} \tag{23}$$

where the wave functions $\{\psi_1, \psi_2\}$ are given by (7). As a consequence, the component of $\hat{A}^S$ in the magnetic frame (X, Y, Z) can be expressed as

$$\begin{aligned} A^S_{Xk} &= \mu_N g_N \mu_B g_e \langle r^{-3}\rangle\{a^2\langle\phi_X|\tau^{\Omega}_{kX}|\phi_X\rangle - b^2\langle\phi_Y|\tau^{\Omega}_{kX}|\phi_Y\rangle \\ &\quad - c^2\langle\phi_Z|\tau^{\Omega}_{kX}|\phi_Z\rangle + 2ab\langle\phi_X|\tau^{\Omega}_{kY}|\phi_Y\rangle + 2ac\langle\phi_X|\tau^{\Omega}_{kZ}|\phi_Z\rangle\}, \\ A^S_{Yk} &= \mu_N g_N \mu_B g_e \langle r^{-3}\rangle\{a^2\langle\phi_X|\tau^{\Omega}_{kY}|\phi_X\rangle - b^2\langle\phi_Y|\tau^{\Omega}_{kY}|\phi_Y\rangle \\ &\quad + c^2\langle\phi_Z|\tau^{\Omega}_{kY}|\phi_Z\rangle - 2ab\langle\phi_X|\tau^{\Omega}_{kX}|\phi_Y\rangle - 2bc\langle\phi_Y|\tau^{\Omega}_{kZ}|\phi_Z\rangle\}, \\ A^S_{Zk} &= \mu_N g_N \mu_B g_e \langle r^{-3}\rangle\{a^2\langle\phi_X|\tau^{\Omega}_{kZ}|\phi_X\rangle + b^2\langle\phi_Y|\tau^{\Omega}_{kZ}|\phi_Y\rangle \\ &\quad - c^2\langle\phi_Z|\tau^{\Omega}_{kZ}|\phi_Z\rangle - 2ac\langle\phi_X|\tau^{\Omega}_{kX}|\phi_Z\rangle - 2bc\langle\phi_Y|\tau^{\Omega}_{kY}|\phi_Z\rangle\} \\ &(k = X, Y, Z). \end{aligned} \tag{24}$$

Note that

$$\begin{aligned} \mathrm{tr}(\hat{A}^S) &= 2\mu_N g_N \mu_B g_e \langle r^{-3}\rangle\{b^2\langle\phi_Y|\tau^{\Omega}_{ZZ}|\phi_Y\rangle + c^2\langle\phi_Z|\tau^{\Omega}_{YY}|\phi_Z\rangle \\ &\quad - 2bc\langle\phi_Y|\tau^{\Omega}_{YZ}|\phi_Z\rangle\}. \end{aligned} \tag{25}$$

which is in general different from zero. Moreover, in general, $\hat{A}^S$ is not a symmetric tensor. For instance

$$\begin{aligned} A^S_{YX} - A^S_{XY} &= \mu_N g_N \mu_B g_e \langle r^{-3}\rangle 2\{c^2\langle\phi_Z|\tau^{\Omega}_{XY}|\phi_Z\rangle \\ &\quad + 2ab\langle\phi_X|\tau^{\Omega}_{ZZ}|\phi_Y\rangle - ac\langle\phi_X|\tau^{\Omega}_{YZ}|\phi_Z\rangle \\ &\quad - bc\langle\phi_Y|\tau^{\Omega}_{XZ}|\phi_Z\rangle\}. \end{aligned} \tag{26}$$

Summarizing, in the fictitious spin formalism the hyperfine interaction can be expressed in the conventional form $\vec{S}' \cdot \hat{A} \cdot \vec{I}$, with the hyperfine coupling tensor $\hat{A}$ being given by

$$\hat{A} = \hat{A}^L + \hat{A}^S + \hat{A}^F, \tag{27}$$

where the different contributions have been calculated above.

2.4. Quadrupolar interaction

In Mössbauer spectroscopy studies of heme systems, quadrupolar interaction of the first excited ^{57}Fe nuclear level ($I = 3/2$) has to be considered. It is represented by

$$H_q = \vec{I} \cdot \tilde{Q} \cdot \vec{I}, \tag{28}$$

where $\tilde{Q}$ is a traceless second range symmetrical tensor given by

$$\tilde{Q} = \frac{eQ}{2I(2I-1)}\tilde{V}. \tag{29}$$

Here $\tilde{V}$ is the electric field gradient (EFG) tensor at the nucleus, which depends on the electron distribution around it, and Q is the intrinsic quadrupolar moment of the nuclear level.

As $\tilde{Q}$ is a symmetric tensor, there is a coordinate system (x_Q, y_Q, z_Q), in which $\tilde{Q}$ and $\tilde{V}$ are diagonal. In this coordinate system (28) is explicitly given as

$$\begin{aligned} H_Q &= \frac{eQ}{4I(2I-1)}V_{z_Qz_Q} \\ &\quad \times \left\{\left[3I^2_{z_Q} - I(I+1)\right] + \eta\left[I^2_{x_Q} - I^2_{y_Q}\right]\right\}, \end{aligned} \tag{30}$$

where the asymmetry parameter:

$$\eta = \frac{V_{x_Qx_Q} - V_{y_Qy_Q}}{V_{z_Qz_Q}}, \tag{31}$$

which is a measure of the departure of EFG of axial symmetry, has been introduced. By imposing $0 \le \eta \le 1$ the canonical ordering of the principal quadrupolar axes (x_Q, y_Q, z_Q) is achieved.

In the absence of applied magnetic field, H_Q induces a splitting of a $I = 3/2$ nuclear level into two doublets with an energy separation given by

$$\Delta E_Q = \frac{1}{2}eQV_{z_qz_q}\sqrt{1 + \frac{1}{3}\eta^2}. \tag{32}$$

This splitting is directly measured in the Mössbauer spectra taken in the absence of applied magnetic field [1,2].

Two contributions must be considered when calculating the EFG [8,21]. The first is the valence contribution $\tilde{V}_v$, which is due to the non-spherical distribution of the valence electrons. The second is the lattice contribution $\tilde{V}_l$, which is due to the spatial distribution of the neighbourhood charges. The latter is strictly zero for a nucleus environment with cubic symmetry. Otherwise it can give a non-zero contribution. The $\tilde{V}_l$ contribution can be estimated considering homologous systems with a metal having

a closed shell electronic configuration, since in this case we have $\tilde{V}_v = 0$. On the other hand, the valence contribution is given by

$$V_{ij} = e\int_{R^3} \rho_c(\vec{r})\frac{3x_i x_j - r^2\delta_{ij}}{r^5}\,d^3\vec{r}, \tag{33}$$

where $\rho_c(\vec{r})$ corresponds to the charge density associated with the unpaired electron. In the case we are considering $\rho_c(\vec{r})$ is given by (A.17). Using (21) it follows that

$$V_{ij} = e\langle r^{-3}\rangle_q \left\{a^2\int \phi_X^2(\Omega)\tau_{ij}^{\Omega}(\Omega)\,d\Omega + b^2\int \phi_Y^2(\Omega)\tau_{ij}^{\Omega}(\Omega)\,d\Omega + c^2\int \phi_Z^2(\Omega)\tau_{ij}^{\Omega}(\Omega)\,d\Omega\right\}. \tag{34}$$

In principle, the $\langle r^{-3}\rangle_q$ values should coincide with $\langle r^{-3}\rangle$ derived from other properties, for instance from the hyperfine interaction. In practice a relation such as

$$\langle r^{-3}\rangle_q = (1 - R_q)\langle r^{-3}\rangle \tag{35}$$

holds, where the factor R_q comes from the closed shell electron contribution. This factor can be either positive (shielding) or negative (antishielding) and represents the distortion of these closed shells by the active electron [21].

The EFG tensor calculated by (34) can be diagonalized to obtain the asymmetry parameter η and the quadrupolar splitting ΔE_Q that can be compared with the experimental values.

3. A particular case in low-spin heme systems

As we have pointed out before, one of the magnetic axes is close to the normal to the porphyrin plane, namely the z-molecular axis, for many studied low-spin heminic systems. In such a case this axis is chosen as the magnetic Z-axis and the orientation of the magnetic axes is given by the angle γ (see Fig. 1). Consequently, the Ω matrix takes the form:

$$\Omega = \begin{pmatrix} \cos\gamma & -\sin\gamma & 0 \\ \sin\gamma & \cos\gamma & 0 \\ 0 & 0 & 1 \end{pmatrix} \tag{36}$$

and the orbitals $\{\phi_X, \phi_Y, \phi_Z\}$ are given by

$$\phi_X = \cos\gamma d_{yz} - \sin\gamma d_{xz} = d_{y'z},$$
$$\phi_Y = \sin\gamma d_{yz} + \cos\gamma d_{xz} = d_{x'z}, \qquad \phi_Z = d_{xy}, \tag{37}$$

where the x' and y' axes are obtained from the molecular x- and y-axes by a rotation of angle γ (see Fig. 3). We will call the set of axes (x', y', z') with $z' \equiv z$ the electronic reference frame. Note that in order to preserve the condition that the z axes of the three relevant frames are collinear, which is very convenient in the description of these systems, sometimes the canonical condition $0 \le V \le 2|\Delta|/3$ is not fulfilled.

With these orbital wave functions, the spin contribution to the hyperfine tensor can be explicitly obtained by using (24). The

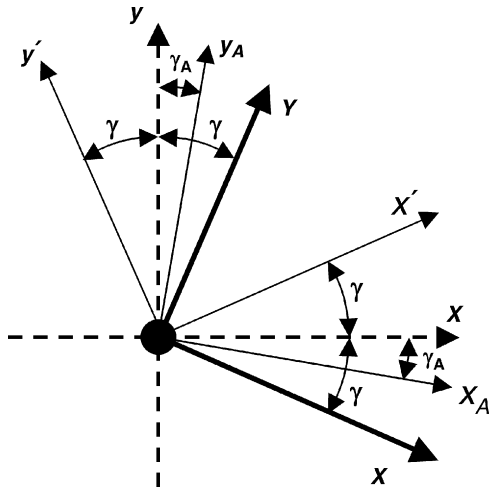

Fig. 3. Outline of the molecular (x and y), magnetic (X and Y), electronic (x' and y') and hyperfine (x_A and y_A) axes in the case of the low-spin heme system analyzed in the text. The $z \equiv Z \equiv z' \equiv z_A$ axes are normal to the plane. The angles γ and γ_A, that define the orientation of the magnetic axes and hyperfine axes, respectively, are also shown.

components of $\hat{A}^S$ in the magnetic axes are given by

$$A_{XX}^S = g_N\mu_N g_e\mu_B\langle r^{-3}\rangle\tfrac{2}{7}\{-2a^2 - b^2 - c^2 + 3ab + 3ac + 3(a-b)^2\sin^2 2\gamma\},$$
$$A_{YY}^S = g_N\mu_N g_e\mu_B\langle r^{-3}\rangle\tfrac{2}{7}\{a^2 + 2b^2 + c^2 - 3ab - 3bc - 3(a-b)^2\sin^2 2\gamma\},$$
$$A_{ZZ}^S = g_N\mu_N g_e\mu_B\langle r^{-3}\rangle\tfrac{2}{7}\{a^2 + b^2 + 2c^2 - 3ac - 3bc\},$$
$$A_{XY}^S = A_{YX}^S = -g_N\mu_N g_e\mu_B\langle r^{-3}\rangle\tfrac{6}{7}(a-b)^2\sin 2\gamma\cos 2\gamma,$$
$$A_{XZ}^S = A_{ZX}^S = A_{YZ}^S = A_{ZY}^S = 0 \tag{38}$$

and, including the orbital and Fermi contributions, which are diagonal in the magnetic axes (A.17), the complete hyperfine coupling tensor can be given by

$$A_{XX} = P\{-4kbc - (1+\kappa)(a^2 - b^2 - c^2) + \tfrac{3}{7}(a^2 - 3b^2 - 3c^2) + \tfrac{6}{7}a(b+c) + \tfrac{6}{7}(a-b)^2\sin^2 2\gamma\},$$
$$A_{YY} = P\{4kac - (1+\kappa)(a^2 - b^2 + c^2) + \tfrac{3}{7}(3a^2 - b^2 + 3c^2) - \tfrac{6}{7}b(a+c) - \tfrac{6}{7}(a-b)^2\sin^2 2\gamma\},$$
$$A_{ZZ} = P\{4kab - (1+\kappa)(a^2 + b^2 - c^2) + \tfrac{3}{7}(3a^2 + 3b^2 - c^2) - \tfrac{6}{7}c(a+b)\},$$
$$A_{XY} = A_{YX} = -P\tfrac{6}{7}(a-b)^2\sin 2\gamma\cos 2\gamma,$$
$$A_{XZ} = A_{ZX} = A_{YZ} = A_{ZY} = 0 \tag{39}$$

with

$$P = g_N\mu_N g_e\mu_B\langle r^{-3}\rangle. \tag{40}$$

Expression (39) coincides with those cited by Walker if the angle γ is a multiple of $\pi/2$, for them we have $\sin 2\gamma = 0$ [1,10,13,22,23]. This happens when the magnetic axes (X, Y,

Z) coincide with the molecular axes (x, y, z), i.e., when the Fe–N bonding directions are principal axes of the g tensor and counter-rotation does not take place.

If P and κ were known the hyperfine coupling coefficient (39) can be computed as a function of the magnetic axes orientation given by the angle γ using the values of the a, b, c parameters obtained from the EPR data Then, a comparison with the observed hyperfine splitting lets us determine the magnetic axes orientation and, in principle, could provide a way of deciding between the two possible solutions for the a, b, c parameters. We will use this strategy in the next section.

Moreover, the hyperfine coupling tensor turns out to be symmetric with our identification of the of the spin states $\{\psi_1 \leftrightarrow |+\rangle, \psi_2 \leftrightarrow |-\rangle\}$. As Abragam and Bleaney discussed [20] this is not an essential property of the hyperfine tensor when a Kramers doublet is described using the $S = \frac{1}{2}$ spin formalism. However, with our particular election it can be transformed in a diagonal form. Its form depicted in (39) indicates that one of its principal axes (z_A) coincides with the molecular z-axis and the other two, x_A and y_A, are in the heme plane being γ_A the angle that the x_A makes with the molecular x-axis (see Fig. 3). In general γ_A differs from γ.

The valence contribution to the EFG can also be calculated for this particular case. The term in (34) is evaluated using the orbital wave functions (37), giving

$$
\begin{aligned}
V_{XX} &= -e\langle r^{-3}\rangle_q \tfrac{1}{7}\{(a^2+b^2-2c^2)+3(a^2-b^2)\cos 4\gamma\},\\
V_{YY} &= -e\langle r^{-3}\rangle_q \tfrac{1}{7}\{(a^2+b^2-2c^2)-3(a^2-b^2)\cos 4\gamma\},\\
V_{ZZ} &= e\langle r^{-3}\rangle_q \tfrac{2}{7}(a^2+b^2-2c^2),\\
V_{XY} &= V_{YX} = -e\langle r^{-3}\rangle_q \tfrac{3}{7}(a^2-b^2)\sin 4\gamma,\\
V_{XZ} &= V_{ZX} = V_{YZ} = V_{ZY} = 0.
\end{aligned}
\tag{41}
$$

The EFG tensor is diagonal in the electronic axes (x', y', z') and its principal values are

$$
\begin{aligned}
V_{x'x'} &= e\langle r^{-3}\rangle_q \tfrac{2}{7}(-2a^2+b^2+c^2),\\
V_{y'y'} &= e\langle r^{-3}\rangle_q \tfrac{2}{7}(a^2-2b^2+c^2),\\
V_{z'z'} &= e\langle r^{-3}\rangle_q \tfrac{2}{7}(a^2+b^2-2c^2).
\end{aligned}
\tag{42}
$$

Thus, the asymmetry parameter η is given by the expression:

$$\eta = -3\frac{a^2-b^2}{a^2+b^2-2c^2}, \tag{43}$$

which coincides with those already published by Lang and Marshall [2]. Moreover, the quadrupolar splitting becomes

$$\Delta E_Q = \frac{2}{7}e^2 Q\langle r^{-3}\rangle_q \sqrt{1-3(a^2b^2+b^2c^2+c^2a^2)}. \tag{44}$$

Note that in general the value of the asymmetry parameter given by (43) does not correspond to a canonical ordering of the quadrupolar axes. As we will see later, in many of the studied systems the dominant coefficient in the ground state wave function is a and, consequently, the z_q-axis coincides with the x'-axis. In this case we have

$$\eta = 3\frac{b^2-c^2}{2a^2-b^2-c^2}. \tag{45}$$

satisfying $0 \le \eta \le 1$.

When the valence contribution to the quadrupolar coupling tensor is known additional structural information can be obtained. Its principal axes give the orientation of the principal g tensor and a comparison of the calculated asymmetry parameter with the experimental one provides an independent way to verify the coefficients (a, b, c) that define the ground state Kramers doublet.

We also want to note that the particular case we have analyzed here is close to that considered by Oosterhuis and Lang [8] in order to explain the Mössbauer spectrum of $K_3Fe(CN)_6$. The different substitution rule used by these authors when applying the effective $S = \frac{1}{2}$ formalism lead them to obtain a hyperfine coupling tensor which non-diagonal part is skewsymmetric.

4. Analysis of some experimental results

We will use the formerly developed model to analyze some experimental results available in the literature. As we have indicated in the introduction, there are several review papers that collect data of some hemeproteins as well as model compounds [1,3,4]. However, as Walker pointed out [1], only partial information exists in some cases. There are also systems with complete EPR and Mössbauer data available, but in these cases the analysis was done using the Taylor formalism under the assumption of common molecular and magnetic frames.

With all these considerations, we collect in Table 1 data from systems where complete experimental information derived in an independent way is available. We also add the results we have obtained by applying the formerly described model to them. We have classified the low-spin Fe^{III} systems according to Walker [1]. Type I corresponds to those systems with very large g_z values (>3.3). Elsewhere in the literature these systems are referred to as HALS. Type II includes those systems in which the highest principal g value is g_z as in Type I, but the g tensor anisotropy is lower than that found in Type I. While Type I systems are associated with an almost perpendicular arrangement of the axial ligands, Type II systems are associated with a practically parallel alignment of them. Type III systems have a practically axial g tensor with the distinguished principal value g_z being the lowest one.

Values of some relevant Fe^{III} properties used in our calculations are collected in Table 2. Substituting the numerical values that are presented in this table in (44), we obtain an expression for the estimation of the quadrupolar splitting without considering the effect of the closed shells as a function of the coefficients (a, b, c) that describe the ground state Kramers doublet:

$$(\Delta E_Q)_{\text{cal}} = 5.96\sqrt{1-3(a^2b^2+b^2c^2+c^2a^2)}\,\text{mm s}^{-1}. \tag{46}$$

This expression is equivalent to

$$\tfrac{1}{2}QV_{z'z'} = (a^2+b^2-2c^2)\times 2.98\,\text{mm s}^{-1}. \tag{47}$$

Table 1
Data of different low-spin Fe(III) heme compounds and results of their analysis

Compound	$g_x, g_y, g_z, \sum g_i^2$	δ (mm s^{-1}), ΔE_Q (mm s^{-1}), η	A_X^{ef} (T), A_Y^{ef} (T), A_Z^{ef} (T) (exp)	a, b, c, k	Δ/ζ, V/ζ, V/Δ	P (T), P/P_0, κ	γ (°), γ_A (°)	A_X^{ef} (T), A_Y^{ef} (T), A_Z^{ef} (T) (cal)	ΔE_Q (mm s^{-1}), η, η_x	$(\Delta E_Q)_{ex}/(\Delta E_Q)_c$	Reference
Type I											
$[PPIXFe(Py)_2]^+$ (I-1)	−0.6, 1.39, 3.64, 15.54	0.25, 1.95, −0.64	35.0, 35.0, 86.0	0.735, 0.616, 0.284, 1.085	1.66, 0.22, 0.13	53.6, 0.75, 0.40	45.0, 45.0	35.0, 35.0, 86.0	2.41, −0.64	0.81	[9]
Mb-CN (I-2)	0.93, 1.89, 3.45, 16.34	0.16, 1.46, –	32.0, 17.0, 76.0	0.895, 0.417, 0.158, 1.037	3.36, 0.94, 0.28	57.8, 0.81, 0.37	8.5, 12.2	32.0, 17.0, 76.0	4.25, −2.03, −0.32	0.34	[9]
H(Py)(CN) (I-3)	0.93, 1.89, 3.45, 16.34	0.34, 1.24, −2.03	34.7, 26.8, 86.9	0.895, 0.417, 0.158, 1.037	3.36, 0.94, 0.28	63.6, 0.89, 0.29	0.0, 0.0	30.0, 22.8, 88.6	4.25, −2.03, −0.32	0.29	[9]
$[((OMe)_2)_4TPPFe(N\text{-}MeIm)_2]^+$ (I-4)	0.89, 1.82, 3.45, 16.01	0.22, 1.84, −1.3	33.3, 18.0, 103.8	0.889, 0.430, 0.156, 1.011	3.46, 0.88, 0.26	76.3, 1.06, 0.32	23.3, 31.1	33.3, 18.0, 103.8	4.17, −1.96, −0.35	0.44	[10]
$[((OMe)_2)_4TPPFe(4\text{-}NMe_2Py)_2]^+$ (I-5)	0.96, 1.80, 3.44, 15.99	0.2, 1.6, −2.0	33.1, 15.3, 82.5	0.895, 0.423, 0.143, 1.006	3.83, 0.91, 0.24	62.8, 0.87, 0.35	6.4, 9.5	33.1, 15.3, 82.5	4.26, −1.99, −0.34	0.38	[10]
$[TPPFe(2\text{-}MeImH)_2]^{+b}$ (I-6)	0.82, 1.87, 3.41, 15.80	0.21, 1.71, −2.0	34.7, 22.0, 81.0	0.884, 0.433, 0.176, 1.001	2.97, 0.88, 0.27	62.6, 0.87, 0.36	0.0, 0.0	34.6, 21.6, 81.1	4.09, −1.96, −0.35	0.42	[1,24]
CCP-N_3 (I-7)	1.08, 1.81, 3.33, 15.53	0.28, 2.45, −2.08	26.0, 8.5, 75.7	0.902, 0.402, 0.132, 0.960	4.18, 1.00, 0.24	62.1, 0.87, 0.34	24.0, 36.0	26.0, 8.5, 75.7	4.42, −2.09, −0.30	0.55	[9]
Type II											
Cyt c_2 from *Rhodospirillum rubrum* (II-1)	1.23, 2.11, 3.13, 15.76	0.25, 2.26, −1.5	35.0, 25.0, 62.5	0.927, 0.340, 0.158, 0.976	3.08, 1.33, 0.43	60.2, 0.84, 0.29	0.0, 0.0	33.5, 21.0, 64.6	4.73, −2.41, −0.17	0.48	[16]
$[\{(OMe)_2\}_4]TPPFe(N\text{-}MeIm)_2]^+$ (II-2)	1.49, 2.252, 2.989, 16.23	0.23, 2.05, −2.22	40.3, 14.6, 53.0	0.954, 0.267, 0.135, 1.041	3.39, 1.83, 0.54	64.8, 0.90, 0.41	15.4, 28.3	40.3, 14.6, 53.0	5.16, −2.66, −0.09	0.40	[10]
$[TPCFe(ImH)_2]^+$ (II-3)	1.49, 2.29, 2.92, 15.99	0.27, 2.36, −2.92	34.0, 0.2 57.0	0.954, 0.261, 0.146, 1.010	3.01, 1.90, 0.63	73.7, 1.03, 0.39	31.4, 54.7	29.6, 12.8, 56.6	5.17, −2.70, −0.08	0.46	[10]
$[\{(OMe)_2\}_4]TPPFe(N\text{-}MeIm)_2]^+$ (II-4)	1.62, 2.30, 2.85, 16.04	0.26, 2.16, –	33.6, 16.5, 50.0	0.967, 0.225, 0.124, 1.049	3.51, 2.25, 0.64	65.9, 0.62, 0.33	21.0, 41.51	33.6, 16.5, 50.0	5.37, −2.78, −0.06	0.40	[10]
$[OMTPPFe(1\text{-}MeIm)_2]^{+c}$ (II-5)	1.58, 2.30, 2.83, 15.79	−, 2.15, −1.83	41.6, 17.7, 44.6	0.963, 0.235, 0.135, 1.000	3.16, 2.15, 0.68[d]	62.4, 0.87, 0.35	4.6, 9.0	41.6, 17.7, 44.6	5.31, −2.77, −0.06	0.41	[25]
MbN_3 (II-6)	1.71, 2.22, 2.80, 15.69	0.24, 2.25, −2.79	23.7, 18.6, 39.4	0.974, 0.206, 0.096, 1.042	4.76, 2.44, 0.51	59.5, 0.83, 0.37	30.3, 68.4	23.7, 18.6, 39.4	5.50, −2.79, 0.05	0.41	[9]
$[OMTPPFe(1\text{-}MeIm)_2]^{+e}$ (II-7)	1.54, 2.51, 2.71, 16.02	0.28, 2.80, −2.03	42.2, 23.6, 50.2	0.961, 0.213, 0.177, 1.019	1.89, 2.47, 1.31[d]	86.1, 1.20, 0.39	25.2, 45.0	42.2, 23.6, 50.2	5.28, −2.91, −0.02	0.53	[25]
Heme *c* of *T. denitrificans* cytochrome cd_1 nitrite reductase (II-8)	1.70, 2.43, 2.50, 15.04	−, 1.70, −2.0	12.5, 12.0, 32.	0.974, 0.168, 0.153, 0.909	1.96, 3.19, 1.63[d]	56.3, 0.78, 0.18	32.9, 69.7	12.5, 12.0, 32.	5.50, −2.97, −0.01	0.31	[26]
$[TPCFe(ImH)_2]^+$ (II-9)	1.78, 2.39, 2.47, 14.98	0.27, 2.36 −2.92	46.3, 19.5, 30.7	0.981, 0.145, 0.128, 0.942	2.41, 3.69, 1.53[d]	73.7, 1.03, 0.33	13.7, 30.1	46.0, 22.8, 28.5	5.63, −2.97, −0.01	0.42	[10]
P450cam (II-10)	1.91, 2.26, 2.45, 14.76	0.38, 2.85, −1.80	45.0, 10.2, 19.1	0.993, 0.102, 0.066, 1.154	5.68, 5.10, 0.90[d]	57.0, 0.80, 0.36	5.9, 14.4	45.0, 10.2, 19.1	5.83, −2.96, −0.01	0.49	[27]
P450cam(2-PhImH) (II-11)	1.91, 2.25, 2.41, 14.52	0.36, 2.85 −2.8	44.0, 9.6, 17.0	0.992, 0.102, 0.069, 1.065	5.28, 5.14, 0.97[d]	56.3, 0.79, 0.35	5.2, 12.9	44.0, 9.6, 17.0	5.82, −2.97, −0.01	0.49	[27]
$TPPFe(3NH_2PzH)_2]^+$ (II-12)	1.87, 2.28, 2.39, 14.41	0.25, 2.5, −3.0	47.6, 6.7, 18.3	0.989, 0.118, 0.093, 0.912	3.60, 4.49, 1.25[d]	61.2, 0.85, 0.37	0.0, 0.0	47.9, 9.4, 15.9	5.76, −2.97, −0.01	0.43	[13]
Type III											
$[OEPFe(t\text{-}BuNC)_2]^+$ (III-1)	−2.28, 2.28, −1.83, 13.74	–, −1.80, –	18.8, 12.2, 36.3	0.126, 0.126, 0.984, 0.694	−4.29, –, –	57.5, 0.80, 0.25	–, –	15.5, 15.5, 36.3	5.68, 0, –	0.32	[28]
$[TPPFe(t\text{-}BuNC)_2]^+$ (III-2)	−2.21, 2.21, −1.93, 13.49	–, −1.89, –	−8.7, 23.0, 34.2	0.080, 0.080, 0.994, 0.742	−6.64, –, –	55.7, 0.79, 0.17	–, –	15.8, 15.8, 34.2	5.85, 0	0.32	[28]
$[TPPFe(2,6\text{-}xylylNC)_2]^+$ (III-3)	−2.2, 2.2, −1.94, 13.44	0.08, −1.99, –	5.5, 5.5, 40.0	0.074, 0.074, 0.995, 0.756	−7.17, –, –	50.7, 0.71, 0.34	–, –	5.5, 5.5, 40.0	5.86, 0, –	0.34	[29]
$[p\text{-}TPPFe(2,6\text{-}xylylNC)_2]^+$ (III-4)	−2.2, 2.2, −1.94, 13.44	0.14, −1.81, –	5.5, 5.5, 40.0	0.074, 0.074, 0.995, 0.756	−7.17, –, –	50.7, 0.71, 0.34	–, –	5.5, 5.5, 40.0	5.86, 0, –	0.31	[29]
$[m\text{-}TPPFe(2,6\text{-}xylylNC)_2]^+$ (III-5)	−2.14, 2.14, 2.14, 13.74	0.12, −1.94, –	2.5, 2.5, 32.0	0.577, 0.577, 0.577, 1.105	–, –, –	11.9, 0.17, 0.75	–, –	12.3, 12.3, 12.3	–, –, –	–	[29]
$TPPPFe(4\text{-}CNPy)_2]^+$ (III-6)	−2.62, 2.62, −0.90, 14.57	0.20, −0.80, –	56.5, 62.9, 0.4	0.308, 0.308, 0.900, 0.901	−1.62, –, –	40.3, 0.56, −0.60[a]	–, –	59.7, 59.7, 0.4	4.26, 0	0.19	[10]

[a] In this case a negative value of κ is obtained. It could indicate that our model is not suitable for it.
[b] The author indicated that the calculated Mössbauer spectra have small sensibility in the A_x value.
[c] The axial ligands are placed parallel.
[d] In this cases the ratio V/Δ is higher than 2/3 and the axes we used are not proper axes.
[e] The axial ligands make a dihedral angle of 19.5°.

Table 2
Some useful values of Fe(III) ion properties

$\langle r^{-3}\rangle_0$	5.724 a.u.[a]
^{57}Fe nucleus, ground state ($I = 1/2$)	
g_N	−0.102[b]
^{57}Fe nucleus, first excited state ($I = 3/2$)	
g_N	0.1806[c]
$\lvert e\rvert Q$	0.18×10^{-24} cm^2[c]
$e^2Q\langle r^{-3}\rangle_q$	242.27 MHz (20.86 mm s^{-1})
$P_0/\mu_N g_N$	71.78 T

[a] From Ref. [30].
[b] From Ref. [8].
[c] From Ref. [31].

To take into account the effects of the shielding parameterized by R_q, and those of the covalent contribution, Lang and Marshall [2] substituted the former expression by

$$\tfrac{1}{2}QV_{z'z'} = (a^2 + b^2 - 2c^2) \times 1.5\,\text{mm s}^{-1} \quad (48)$$

and in this way introduced those effects empirically. This expression has been widely used in order to analyze the nuclear quadrupolar contribution to Mössbauer spectra in these systems [1–3]. We will calculate the quadrupolar splitting with (46) and compare it to the experimental value. This comparison will allow us to obtain an estimation of the shielding contribution.

Let us comment on the data shown in Table 1. The three first columns contain the experimental information about the studied system. In the first column, the principal values of the g tensor (including signs) are displayed together the sum $g_X^2 + g_Y^2 + g_Z^2$. In a purely ionic model, this sum should take a value between 12 and 16, but sometimes the empirical relation $g_X^2 + g_Y^2 + g_Z^2 = 16$ has been used to estimate the lowest principal value of the g tensor when only the other two can be experimentally determined. Values of the isomer shift δ relative to α-Fe at room temperature, the quadrupolar splitting ΔE_Q, and the asymmetry parameter η are found in the next column. The experimental effective hyperfine coupling constants A_X^{ef}, A_Y^{ef}, A_Z^{ef} are also given in the third column. The last columns display the results we have obtained after applying the formerly described model to analyze the experimental data.

At this point we want to recall that, in principle, there are two possible "solutions" derived from the g-values. However, only one of them has been displayed in Table 1. It is this one which turns out to be compatible with the hyperfine data from Mössbauer spectra after applying the procedure outlined below. The other one has been rejected since it is not compatible with these data.

So, in the following column, the values of the coefficients (a, b, c) derived from these experimentally determined principal values of the g tensor are displayed together with the value of the orbital coefficient k, which should be equal to the unity in a pure ionic system. In the next column, the crystal field parameters Δ/ζ and V/ζ and the ratio V/Δ calculated using Taylor's equations are shown. In some Type II cases the ratio V/Δ is higher than 2/3, indicating that we are not working with proper axes. The model does not require using proper axes. It only assumes that one of the principal axes of the g-tensor is normal to the heme plane and the Ω matrix takes the form given in (36).

The effective hyperfine coupling constants A_X^{ef}, A_Y^{ef}, A_Z^{ef} for a magnetic field along one of the principal axes of the g tensor are calculated as

$$A_X^{ef} = [A_{XX}^2 + A_{XY}^2]^{1/2}, \qquad A_Y^{ef} = [A_{YX}^2 + A_{YY}^2]^{1/2},$$
$$A_Y^{ef} = A_{ZZ} \quad (49)$$

in a first-order approximation, where A_{XX}, $A_{XY} = A_{YX}$, A_{YY} and A_{ZZ} are given by (39). Thus, these effective hyperfine coupling constants can be expressed as a function of the P, κ and γ parameters. Using the parameters (a, b, c) given above and fitting (49) to the experimental effective hyperfine coupling constants, values for P, κ and γ are obtained. They are shown in the next two columns. The quotient P/P_0 is also shown, where P_0 is the free ion value of P (see above). Now that we have estimated values for the parameters a, b, c, P, κ and γ, the expression of the hyperfine tensor in the magnetic axes (X, Y, Z) can be calculated. Its diagonalization lets us estimate the angle γ_A, which the principal axis x_A makes with the molecular direction x (see Fig. 3). Values of γ_A are also given in Table 1. In general, γ_A is different from γ. Predicted values for the effective hyperfine coupling constants A_X^{ef}, A_Y^{ef}, A_Z^{ef} are calculated using (49) and also given in Table 1. Their comparison with the experimental ones allows us to evaluate our model.

The calculated quadrupolar splitting $(\Delta E_Q)_c$ and asymmetry parameter η (43) and (44) are shown in the next column. They compare to the experimentally obtained values shown in the second column. When the value of η is higher than one, a value of η_x is given that corresponds to an ordering of the quadrupolar principal axes in such a way that the z_q axis coincides with the x'-axis (see above). Finally, the quotient $(\Delta E_Q)_c/(\Delta E_Q)_{ex}$, which is related to the quadrupolar reduction factor $r_q = 1 - R_q$, see (35), is shown.

It is worth noting that the product $g_x g_y g_z$ is positive in practically all the cases as it was obtained in Cytochrome c_2 from *R. rubrum* [18] and was assumed by Taylor [7]. In only two systems, I-1 and III-5, do we have $g_x g_y g_z < 0$. As can be seen, the ionic approximation is fairly good for these systems as long as the obtained values of k are close to unity. That is particularly true in the case of Type I and Type II complexes, where the values obtained for the hyperfine parameter P are close to its free ion value P_0, but the quotient P/P_0 departs appreciably from unity in Type III complexes. Moreover, in some Type III complexes k departs noticeably from the unity and, perhaps the model could be not applied. In Types I and II complexes the z_Q axis of the quadrupolar interaction is along the x' electronic axis, the quadrupolar interaction being almost axial in the case of Type II complexes. In Type III complexes, the z_Q axis is along the z molecular axis according to the axial symmetry of these systems. In most of the cases asymmetry parameters η calculated from the experimental principal values of the g tensor (Eqs. (43) and (45)) are in good agreement with those obtained experimentally (and appearing in the second column of Table 1). The quadrupolar reduction factor in the last column of Table 1 is between 0.31 and 0.54 for all the systems except one (III-6).

In this case the values obtained from the hyperfine analysis indicate that the model does not fit with this system. Although the empirical estimation of the reduction introduced by Lang and Marshall [2] (around 0.5) is close to those values, it seems that in some cases it can lead to an inaccurate estimation of the effect.

In the past, several analyses of the experimental data have been attempted following diverse methodologies. In a very comprehensive approach, Rhynard et al. [9] took Mössbauer data of many low-spin ferric heme complexes and from them obtained information about the orientation of the g and hyperfine tensor. They parameterized the spectra as a function of the crystal field parameters relative to the spin-orbit coupling constants Δ/ζ and V/ζ, and the Euler angles that give the orientation of the g tensor relative to the molecular axes. The quadrupolar reduction factor $r_q = 1 - R_q$ and the hyperfine parameter P were also varied in the fitting procedure, while a value of $\kappa = 0.35$ was kept constant. The orbital reduction factor k was also allowed to vary in the fitting procedure. We have included in our analysis the data studied by these authors [9] and it is very gratifying that our results show an excellent agreement with those obtained there.

Finally, we want to point out that, unfortunately, no clear X-ray data are available in these low-spin Fe^{III} systems where a complete EPR and Mössbauer information exists. That prevents us relating the information derived above with structural features of the Fe^{III} moiety as the orientation of the axial ligands.

5. Summary

A comprehensive description of the g-tensor together with the hyperfine and quadrupolar interactions with the iron nucleus in low-spin Fe^{III} systems has been given.

It has been proved that the description of the g-tensor as a function of the ground state electronic distribution given by the a, b, c parameters introduced by Taylor [7] also works in a general situation. That prevents getting information about the magnetic axes (and also on the electronic axes) orientation when only EPR data in disorder samples are available.

Moreover, there are two essentially different electronic distributions compatible with conventional EPR data. They can be distinguished by analyzing the hyperfine interaction with the iron nucleus. This provides valuable knowledge about the electronic distribution. Besides the hyperfine interaction can give information about magnetic axes (and consequently on the electronic axes) orientation.

Explicit expressions are given where the orientation of one of the principal axes is known and the orientation of the magnetic axes are defined by only a rotation angle. This situation covers a large number of the low-spin hemic systems reported in the literature.

Acknowledgements

This work was supported by Dirección General de Investigación, Spain (Grant No. BFU2005-07422-C02-02/BMC) and it has been done within the GC DGA program of Gobierno de Aragón (Grupos Consolidados E33 and B18).

Appendix A. $S' = \frac{1}{2}$ fictitious spin description of the ground state doublet

The use of the fictitious spin formalism allows one to describe the behavior of a Kramers doublet in a more compact and simple way. This is done by the identification of the base states $\{\psi_1, \psi_2\}$ of the Kramers doublet with the standard states $\{|+\rangle, |-\rangle\}$ of an $S = \frac{1}{2}$ spin and substitution of each of the operators $\hat{O}$, when restricted to the Kramers doublet, by an equivalent operator $\hat{O}_S$ that is expressed as a function of spin operators. After doing a specific association the observable $\hat{O}$ is substituted in the fictitious spin formalism by

$$\hat{O}_S = O_0 I + \vec{O} \cdot \vec{S}', \tag{A.1}$$

where the real coefficient O_0 and the components O_x, O_y and O_z of the real vector $\vec{O}$ satisfy

$$\langle\psi^+|\hat{O}|\psi^+\rangle = O_0 + \frac{1}{2}O_z, \qquad \langle\psi^-|\hat{O}|\psi^-\rangle = O_0 - \frac{1}{2}O_z,$$
$$\langle\psi^+|\hat{O}|\psi^-\rangle = \frac{1}{2}O_x - \frac{\mathrm{i}}{2}O_y, \qquad \langle\psi^-|\hat{O}|\psi^+\rangle = \frac{1}{2}O_x + \frac{\mathrm{i}}{2}O_y, \tag{A.2}$$

where ψ^+ and ψ^- denote the actual functions (ψ_1, ψ_2) associated to $|+\rangle$ and $|-\rangle$, respectively. Note that decomposition (A.1) is always possible using (A.2) and when $\hat{O}$ is a time-even (time-odd) operator $\vec{O} = 0$ ($O_0 = 0$).

Relation (A.1) can be generalized for a vector operator $\vec{\mathbf{V}}$, to which the spin operator $\vec{\mathbf{V}}_S$ is associated with

$$\vec{\mathbf{V}}_S = \vec{V}_0 + \tilde{\Xi}_V \cdot \vec{S}'. \tag{A.3}$$

In this expression, $\vec{V}_0$ is a real vector and $\tilde{\Xi}_V$ a second rank real tensor with

$$(V_0)_k = \tfrac{1}{2}\{\langle\psi^+|\mathbf{V}_k|\psi^+\rangle + \langle\psi^-|\mathbf{V}_k|\psi^-\rangle\},$$
$$(\Xi_V)_{kx} = 2\,\mathrm{Re}\langle\psi^-|\mathbf{V}_k|\psi^+\rangle, \qquad (\Xi_V)_{ky} = 2\,\mathrm{Im}\langle\psi^-|\mathbf{V}_k|\psi^+\rangle,$$
$$(\Xi_V)_{kz} = \langle\psi^+|\mathbf{V}_k|\psi^+\rangle - \langle\psi^-|\mathbf{V}_k|\psi^-\rangle \quad (k = x, y, z). \tag{A.4}$$

Again, $\tilde{\Xi}_V = 0$ if $\vec{\mathbf{V}}$ is time-even while $\vec{V}_0 = \vec{0}$ if it is time-odd.

Particularly, as the orbital angular moment $\vec{L}$ and the true spin $\vec{S}$ are time-odd vector operators we have the following identification:

$$\vec{J} \leftrightarrow \tilde{\Xi}_J \cdot \vec{S}', \quad J = \mathrm{L}, \mathrm{S}. \tag{A.5}$$

The matrix elements between the ψ^j and ψ^k states of the λ component of $\vec{J}$ are given by

$$(J_\lambda)_{jk} = \langle\psi^j|J_\lambda|\psi^k\rangle = \sum_\mu (\Xi_J)_{\lambda\mu}\tfrac{1}{2}(\sigma_\mu)_{jk}, \tag{A.6}$$

where σ_x, σ_y, and σ_z are the Pauli matrices.

Another type of vector operator used in our model has the form:

$$\vec{V} = \hat{\tau} \cdot \vec{J} \quad (J = \mathrm{L}, \mathrm{S}), \tag{A.7}$$

where $\hat{\tau}$ is a time-even second rank tensor operator. For instance, it could be a second rank tensor operator that only depends on

the space electron coordinates. In this case, the matrix elements of the $\hat{\tau}$ components are given by

$$(\tau_{\mu\nu})_{jk} = T_{\mu\nu}\delta_{jk}, \tag{A.8}$$

with

$$T_{\mu\nu} = \langle\psi^+|\tau_{\mu\nu}|\psi^+\rangle = \langle\psi^-|\tau_{\mu\nu}|\psi^-\rangle = \langle\tau_{\mu\nu}\rangle, \tag{A.9}$$

because this matrix element does not depend on the chosen state within the Kramer doublet.

Since $\vec{\mathbf{V}}$ is a time-odd vector operator ($\hat{\tau}$ is time-even and $\vec{J}$ is time-odd), in the fictitious spin formalisms this translates to

$$\vec{\mathbf{V}}_S = \tilde{\Xi}_V \cdot \vec{S}', \tag{A.10}$$

with the $\tilde{\Xi}_V$ tensor depending on the vector operator $\vec{V}$. The question now is to look for the conditions allowing us to express $\tilde{\Xi}_V$ as a function of $\tilde{\Xi}_J$ (A.5) and $\tilde{T}$ (A.9). Note that

$$J_\lambda|\psi^k\rangle = \sum_{k'}(J_\lambda)_{k'k}|\psi^{k'}\rangle + |\chi^k_\lambda\rangle, \tag{A.11}$$

where $|\chi^k_\lambda\rangle$ indicates the part of $J_\lambda|\psi^k\rangle$ orthogonal to the Kramers doublet.Consequently, using (A.6) and (A.9) the matrix element of (A.7) between the ψ^j and ψ^k states are given by

$$\begin{aligned}(V_\lambda)_{jk} &= \sum_\mu T_{\lambda\mu}(J_\mu)_{jk} + \sum_\mu \langle\psi^j|\tau_{\lambda\mu}|\chi^k_\mu\rangle \\ &= \sum_\mu\sum_\nu T_{\lambda\mu}(\Xi_J)_{\mu\nu}\frac{1}{2}(\sigma_\nu)_{jk} + \sum_\mu\langle\psi^j|\tau_{\lambda\mu}|\chi^k_\mu\rangle.\end{aligned} \tag{A.12}$$

In particular, when the matrix element of the tensor operator $\hat{\tau}$ between any state in the Kramers doublet and $|\chi^k_\lambda\rangle$ is zero, or in a situation that these matrix elements can be neglected, it follows that

$$\tilde{\Xi}_V = \tilde{T}\cdot\tilde{\Xi}_J. \tag{A.13}$$

It is important to note that the last relation is not true in general because it has to include the contribution due to the last equation in (A.12).

When the $\hat{\tau}$ operator only depends on the spatial electronic coordinates, the $T_{\mu\nu}$ components are given by

$$T_{\mu\nu} = \int_{R^3}\tau_{\mu\nu}(\vec{r})\rho(\vec{r})\,\mathrm{d}^3\vec{r}. \tag{A.14}$$

$\rho(\vec{r})$ being defined by

$$\rho(\vec{r}) = \langle\psi^*\psi\rangle_S, \tag{A.15}$$

where $\langle\cdot\rangle_S$ denotes the integration over the spin variables, that turns out to be independent of the state ψ chosen in the Kramers doublet.

Now let us apply these results to the ground state Kramers doublet defined by the basis function in (7). In this case the function $\rho(\vec{r})$ becomes

$$\rho(\vec{r}) = a^2\phi_X^2 + b^2\phi_Y^2 + c^2\phi_Z^2, \tag{A.16}$$

It is important to realize that some arbitrariness exists in the election of a specific association of the base functions (ψ_1, ψ_2) to the $|+\rangle$ and $|-\rangle$ spinors. For instance using the base functions (7) the state ψ_1 can be associated either to $|+\rangle$ or to $|-\rangle$. Moreover, the sign of the a, b, c coefficients in both ψ_1 and ψ_2, functions can be chosen to be equal or different. Some authors invoke arguments of symmetry of the g-tensor in the limit of cubic and axial symmetry for preferring one of these possibilities. So, McGarvey [14,15] decided on the $\psi_2 \leftrightarrow |+\rangle$ and $\psi_1 \leftrightarrow |-\rangle$ association rule that leads to a cyclic symmetry in the expression of the effective g-factors as a function of the a, b, c coefficients that describe the ground state Kramers doublet and translate the point symmetry of the paramagnetic entity to the effective "g-tensor". The transformation properties of ψ_1 and ψ_2 states under time reversal ($\hat{I}_t\psi_1 = -\psi_2$, $\hat{I}_t\psi_2 = -\psi_1$) [18] are not preserved with this last association.

In order to keep the time reversal behavior of the basis functions we have adopted the following association: $\psi_1 \leftrightarrow |+\rangle$ and $\psi_2 \leftrightarrow |-\rangle$. In this case the spatial symmetry properties are not completely translated to the "g-tensor" (it gives $g_x = -g_y$ in axial symmetry). It is important to recall that only the absolute values of the principal g-factors and the sign of the $g_xg_yg_z$ product are observable. The "g-tensor" is not a true tensor and the signs of each principal g-factor can be not determined experimentally [20].

Then, the $\tilde{\Xi}_L$ and $\tilde{\Xi}_S$ tensors, which are diagonal in the axes (X, Y, Z), are explicitly given by

$$\Xi_L = \begin{pmatrix} -4bc & & \\ & 4ac & \\ & & 4ab \end{pmatrix} \quad \text{and}$$

$$\Xi_S = \begin{pmatrix} a^2-b^2-c^2 & & \\ & a^2-b^2+c^2 & \\ & & a^2+b^2-c^2 \end{pmatrix}. \tag{A.17}$$

On the other hand, as the wave functions $\{\phi_X, \phi_Y, \phi_Z\}$ are given as a linear combination of the standard orbitals $\{d_{yz}, d_{zx}, d_{xy}\}$ of the metal that have a common radial part, $R_{3d}(r)$, the $\rho(\vec{r})$ function can be factorized as

$$\rho(\vec{r}) = |R_{3d}(r)|^2\cdot\rho_\Omega(\theta,\phi), \tag{A.18}$$

where the angular part, $\rho_\Omega(\theta, \phi)$, is obtained taking the angular part of the wave functions $\{\phi_X, \phi_Y, \phi_Z\}$. As these angular parts of $\{\phi_X, \phi_Y, \phi_Z\}$ are second degree harmonic homogeneous polynomials in x/r, y/r and z/r, $\rho_\Omega(\theta, \phi)$ can be given as a linear combination of spherical harmonic functions $Y_{kq}(\theta, \phi)$, with $k = 0, 2, 4$.

Moreover, if $\hat{\tau}$ is a second rank tensor operator that only depends on the radial distance r, the $T_{\mu\nu}$ components are given by

$$T_{\mu\nu} = \int_0^\infty |R_{3d}(r)|^2\tau_{\mu\nu}(r)r^2\,\mathrm{d}r. \tag{A.19}$$

In this case, because of the spherical symmetry of $\hat{\tau}$ the relation $\langle\psi^j|\tau_{\lambda\mu}|\chi^k_\mu\rangle = 0$ is exactly satisfied.

A particular case is when $\hat{\tau}$ is the scalar r^n, where we define

$$\langle r^n \rangle = \int_0^\infty |R_{3d}(r)|^2 r^{n+2}\, \mathrm{d}r \tag{A.20}$$

for the Kramers doublet.

References

[1] F.A. Walker, Coord. Chem. Rev. 185/186 (1999) 471.
[2] G. Lang, W. Marshall, Proc. Phys. Soc. 87 (1966) 3.
[3] V. Schünemann, H. Winkler, Rep. Prog. Phys. 63 (2000) 263.
[4] F.A. Walker, Chem. Rev. 104 (2004) 589.
[5] J.S. Griffith, Nature 180 (1957) 30.
[6] B. Bleaney, M.C.M. O'Brien, Proc. Phys. Soc. B 69 (1956) 1216.
[7] C.P.S. Taylor, Biochim. Biophys. Acta 491 (1977) 137.
[8] W.T. Oosterhuis, T. Lang, Phys. Rev. 178 (1969) 439.
[9] D. Rhynard, G. Lang, K. Spartalian, T. Yonetani, J. Chem. Phys. 71 (1979) 3715.
[10] R. Benda, V. Schünemann, A.X. Trautwein, S. Cai, J.R. Polam, C.T. Waston, T.K. Shokhireva, F.A. Walker, J. Biol. Inorg. Chem. 8 (2003) 787.
[11] M.P. Byrn, B.A. Katz, N.L. Keder, K.R. Levan, C.J. Magurany, K.M. Miller, J.W. Pritt, C.E. Strouse, J. Am. Chem. Soc. 105 (1983) 4916.
[12] N.V. Shokhirev, F.A. Walker, J. Am. Chem. Soc. 120 (1998) 981.
[13] V. Schünemann, A.M. Raitsimring, R. Benda, A.X. Tautwein, T.K. Shokhireva, F.A. Walker, J. Biol. Inorg. Chem. 4 (1999) 708.
[14] B.R. McGarvey, Quim. Nova 21 (1998) 206.
[15] B.R. McGarvey, Coord. Chem. Rev. 170 (1998) 75.
[16] B.H. Huynh, M.H. Emptage, E. Münck, Biochim. Biophys. Acta 534 (1978) 295.
[17] M.H.L. Pryce, Phys. Rev. Lett. 3 (1959) 375.
[18] V. Heine, Group Theory in Quantum Mechanics, Pergamon Press, Oxford, 1960, p. 164.
[19] I. García-Rubio, J.I. Martínez, R. Picorel, I. Yruela, P.J. Alonso, J. Am. Chem. Soc. 125 (2003) 15846.
[20] A. Abragam, B. Bleaney, Electron Paramagnetic Resonance of Transition Ions, Clarendon Press, Oxford, 1970 (Chapter 15).
[21] A. Abragam, B. Bleaney, Electron Paramagnetic Resonance of Transition Ions, Clarendon Press, Oxford, 1970 (Chapter 17).
[22] M.K. Safo, G.P. Gupta, F.A. Walker, W.R. Scheidt, J. Am. Chem. Soc. 113 (1991) 5497.
[23] V. Schünemann, A.X. Trautwein, J. Illerhaus, W. Haehnel, Biochemistry 38 (1999) 8981.
[24] F.A. Walker, B.H. Huynh, W.R. Scheidt, S.R. Osvath, J. Am. Chem. Soc. 108 (1986) 5288.
[25] T. Teschner, A.X. Trautwein, V. Schünemann, L.A. Yatsunyk, F.A. Walker, Hyperfine Interact. 156/157 (2004) 265.
[26] B.H. Huynh, M.C. Lui, J.J.G. Moura, I. Moura, P.O. Ljungdahl, E. Münck, W.J. Payne, H.D. Peck, D.V. der Vartain, J. LeGall, J. Biol. Chem. 257 (1982) 9576.
[27] M. Sharrock, P.G. Debrunner, C. Schulz, J.D. Lipscomb, V. Marshall, I.C. Gunsalus, Biochim. Biophys. Acta 420 (1976) 8.
[28] F.A. Walker, H. Nasri, I. Torowska-Tyrk, K. Mohanrao, C.T. Watson, N.V. Shokirev, P.G. Debrunner, W.R. Scheidt, J. Am. Chem. Soc. 118 (1996) 12109.
[29] G. Simonneaux, V. Schünemann, C. Morice, L. Carel, L. Toupet, H. Winkler, A.X. Trautwein, F.A. Walker, J. Am. Chem. Soc. 122 (2000) 4366.
[30] A. Abragam, B. Bleaney, Electron Paramagnetic Resonance of Transition Ions, Clarendon Press, Oxford, 1970, p. 399.
[31] C.E. Johnson, Proc. Phys. Soc. 92 (1967) 748.